YMTHE, Volume *29*

Supplemental Information

Olaparib Suppresses MDSC Recruitment via SDF1α/CXCR4 Axis to Improve the Anti-tumor Efficacy of CAR-T Cells on Breast Cancer in Mice

Ruixin Sun, Hong Luo, Jingwen Su, Shengmeng Di, Min Zhou, Bizhi Shi, Yansha Sun, Guoxiu Du, Honghong Zhang, Hua Jiang, and Zonghai Li

SUPPLEMENTARY MATERIALS AND METHODS

Virus production

Retroviruses were obtained by transfection of 80% confluent 293T cells with 806-28Z CAR and packaging plasmid *p*CL-Eco using poly ethylenimine (PEI). Retroviruses were produced by co-transfection of *p*MSCV-EGFR*v*III together with the packaging plasmid *p*CL-Eco into 80% confluent 293T cells using PEI. Viruses were harvested 48h later and filtered through a 0.45 μm filter unit (Millipore, USA) to remove cell debris.

Murine EGFR*v*III Construction

A murine homolog of the human EGFR*v*III mutation was created by using cDNA sequences spanning the murine EGFR according to report. Briefly, the cDNA sequences cloned into *p*WPT vector to construct the recombinant murine EGFR*v*III. Mouse EGFR*v*III sequences were generated by delete exon 2–7 of mouse EGFR and insert a human EGFR 806 epitope (Amino acids 287–302, CGADSYEMEEDGVRK C) after exon 1. Replication-defective lentiviral vectors containing the recombinant murine EGFR*v*III were then generated by 293T packaging cell lines and used to transfect 4T1 and E0771 cells. Transfected cells were incubated with ch806 Ab followed with FITC-labeled goat anti-human IgG, then positive cells were sorted by flow cytometry. Mouse breast cancer cells E0771EGFR*v*III and 4T1EGFR*v*III cells were constructed by using a lentivirus transfection system.

Proliferation Analysis

Tumor cells and CAR-T cells were plated at 10^4 cells/well in 96-well plates with different concentrations of olaparib or veliparib (0, 0.5 ng/mL, 5 ng/mL, 50 ng/mL, 500 ng/mL, 5 μg/mL). The cell proliferation was analyzed by CCK8 kits at 48h.

Animal experiments

The 4–6 weeks old C57BL/6 mice were bought from Shanghai Sippr BK laboratory animal Co. Ltd. All animal experiments were performed according to protocols approved by the Shanghai Cancer Institute Experimental Animal Care Commission. 5×10^5 EGFR*v*III-positive tumor cells were inoculated into the forth inguinal mammary fat pads of C57BL/6 mice. When the tumor volume reached 120mm^3 (day 14), tumor-bearing mice were randomly grouped (n=6). Mice were administrated with various concentrations of olaparib (10mg/kg, 50mg/kg or 100mg/kg) for 10 days (discontinuous: 5 days consecutively, 2 days off). Then, tumor-bearing mice received tail vein injection of 5×10^6 CAR-T cells in sterile PBS while the control group received 5×10^6 untransduced T (UTD) cells at day 21. Tumor growth was measured twice a week. The tumor volumes were calculated using the following formula: Tumor volumes=length×$width^2$/2. Lack of survival was defined as death or tumor size > 2000 mm^3.

Flow cytometry

To evaluate the impact of olaparib on exhaustion, memory T cells and proliferation of CAR-T cells in the presence of antigen-positive or antigen-negative target cells, EGFR*v*III-positive tumor cells were pre-treated with or without various concentrations of olaparib for 24 h. Then CAR-T cells were labeled with CellTrace Violet, and then, 1×10^5 CellTrace-labeled CAR-T cells were incubated with 1×10^5 EGFR*v*III-positive tumor cells in the presence of various concentrations of olaparib for 24 h. The cells were stained with antibodies against CD3, CD4, CD8, CD44, CD62L, PD1, TIM3 and LAG3 according to the manufacturer's instructions and determined by flow cytometry.

MDSCs Suppression Assays

MDSCs were isolated via Ly6G magnetic selection from bone marrow of healthy mice by using the myeloid-derived suppressor cell isolation kit. To determine whether MDSCs decrease the anti-tumor activity of CAR-T cells *in vitro*, the specific lytic function of CAR-T cells on target cells was examined in the presence of MDSCs. CAR-T cells and target cells were co-cultured at an E:T ratio of 1:1. Isolated MDSCs were added at varying MDSCs:CAR-T cells ratios (1:3, 1:1, 3:1) in E-plate at 37 °C for 18h. Th cytotoxicity was assessed by RTCA.The cytotoxicity of CAR-T cells was analyzed using a standard formula provided in the manual.

Chemotaxis Assay *in vitro*

To determine the effects of olaparib on CAFs-induced chemotaxis of MDSCs, NIH3T3 cells were induced into CAFs by harvested after stimulation with TGFβ for 16 h. The CAFs were treated with 0 or 1μM olaparib for 48h and collected the cell culture supernatants. MDSCs cells (2×10^5) (isolated from bone marrow) were added in the upper chamber and the cell culture supernatants of CAFs from each treatment group were added in the lower chamber. The chamber aperture is 3μm. The cell number in the lower chamber was counted at 2h and 6h. To clarify the effects of olaparib on CXCR4-dependent chemotaxis of MDSCs, MDSCs (2×10^5) (isolated from bone marrow) treated with 0, 1μM olaparib or DMSO for 24 were added in the upper chamber and the cell culture supernatants of CAFs were added in the lower chamber. The chamber aperture is 3μm. The cell number in the lower chamber was counted at 2h and 6h.

***In vivo* and *in vitro* Toxic Effect of olaparib on MDSCs**

To evaluate the direct toxic effect of olaparib on MDSCs, the MDSCs isolated from bone marrow were treated with olaparib *in vitro*. The MDSCs were plated at 10^4 cells/well in 96-well plates with different concentrations of olaparib (0, 0.5 ng/mL, 5 ng/mL, 50 ng/mL, 500 ng/mL and 5 μg/mL). The cell proliferation of MDSCs was analyzed by CCK8 kits at 24h.

The 4–6 weeks old C57BL/6 and BALB/c mice were bought from Shanghai Sippr BK laboratory animal Co. Ltd. All animal experiments were performed according to protocols approved by the Shanghai Cancer Institute Experimental Animal Care Commission. 1×10^6 EGFR*v*III-positive tumor cells were inoculated into the forth inguinal mammary fat pads of C57BL/6 and BABL/c mice. When the tumor volume reached 120mm^3 (day 14), mice were randomly grouped and administrated intraperitoneally with 10mg/kg or 50mg/kg dose of olaparib for 10 days. PBS was served as negative control. After two weeks, the percentages of MDSCs from blood, spleen and bone marrow of mice were determined by flow cytometry.

The separation and culture of tumor-derived CAFs

The EGFR*v*III-positive tumor cells were into mammary fat pads of C57BL/6 and BALB/c mice. After three weeks, mammary tissues near the tumors were isolated, digested with collagenase I, collagenase IV and trypsin, and plated on dishes for culture. Cells grew in two weeks and CAFs were isolated by monoclonal culture.

SUPPLEMENTARY FIGURE AND FIGURE LEGENDS

Fig. S1

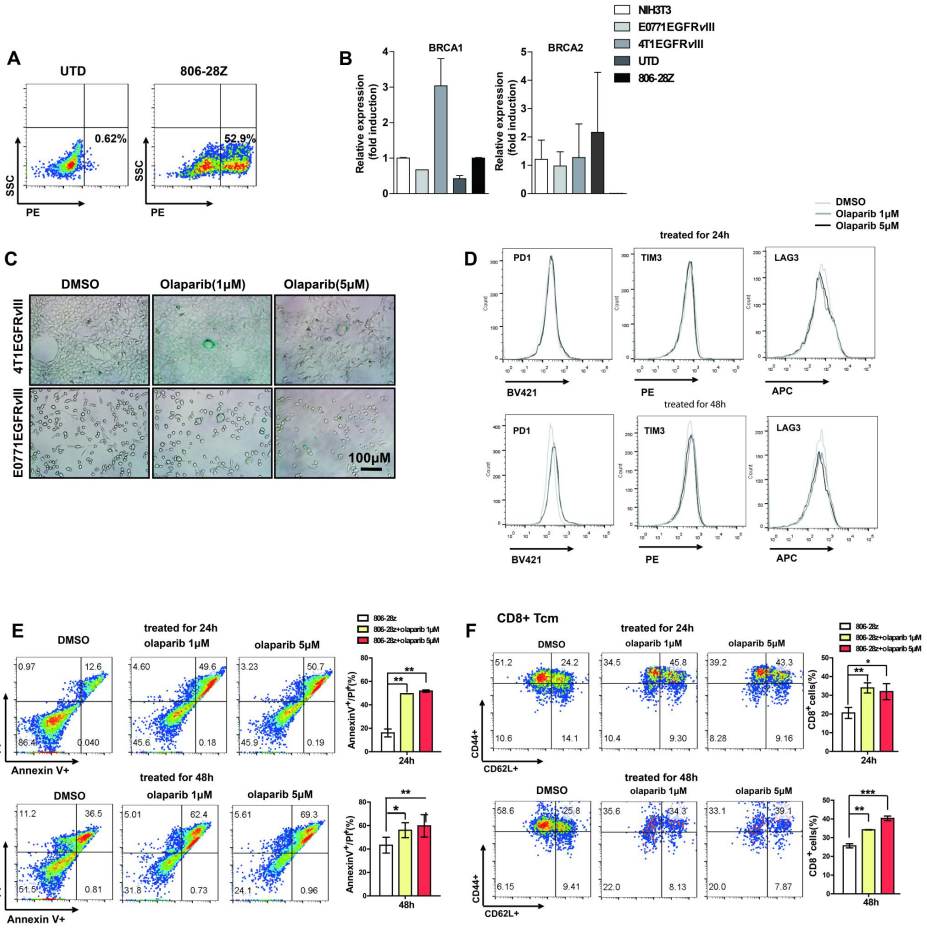

Fig. S1 The effect of olaparib on the phenotype of CAR-T cells

(A) The transduction efficiency of 806-28Z CAR on splenic T cells derived from BABL/c determined by flow cytometry. (B) The mRNA expression of *BRCA1* and *BRCA2* in 4T1EGFR*v*III, E0771EGFR*v*III, NIH3T3, mouse T cells and CAR-T cells. (C) The β-galactosidase staining of E0771EGFR*v*III and 4T1EGFR*v*III cells treated with 0,1μM olaparib or 5μM olaparib for 48h. Scale bars, 100μm. (D) The expression of PD1, TIM3 and LAG3 of CAR-T cells treated with 0, 1μM or 5μM olaparib for 24h or 48h. (E) The representative flow cytometry plots results showing the frequencies of PI^+ and Annexin V^+ CAR-T cells after treated with 0,1 or 5μM olaparib for 24h or 48h. (F) The percentages of CAR-T cells expressing the relevant markers of T_{cm} ($CD44^+CD62L^+$) in $CD8^+$ T cells after treated with 0, 1μM or 5μM olaparib for 24h or 48h, determined by flow cytometry. All data are presented as the mean±SEM of triplicate experiments. **p*<0.05, ***p*<0.01, ****p*<0.001.

Fig. S2

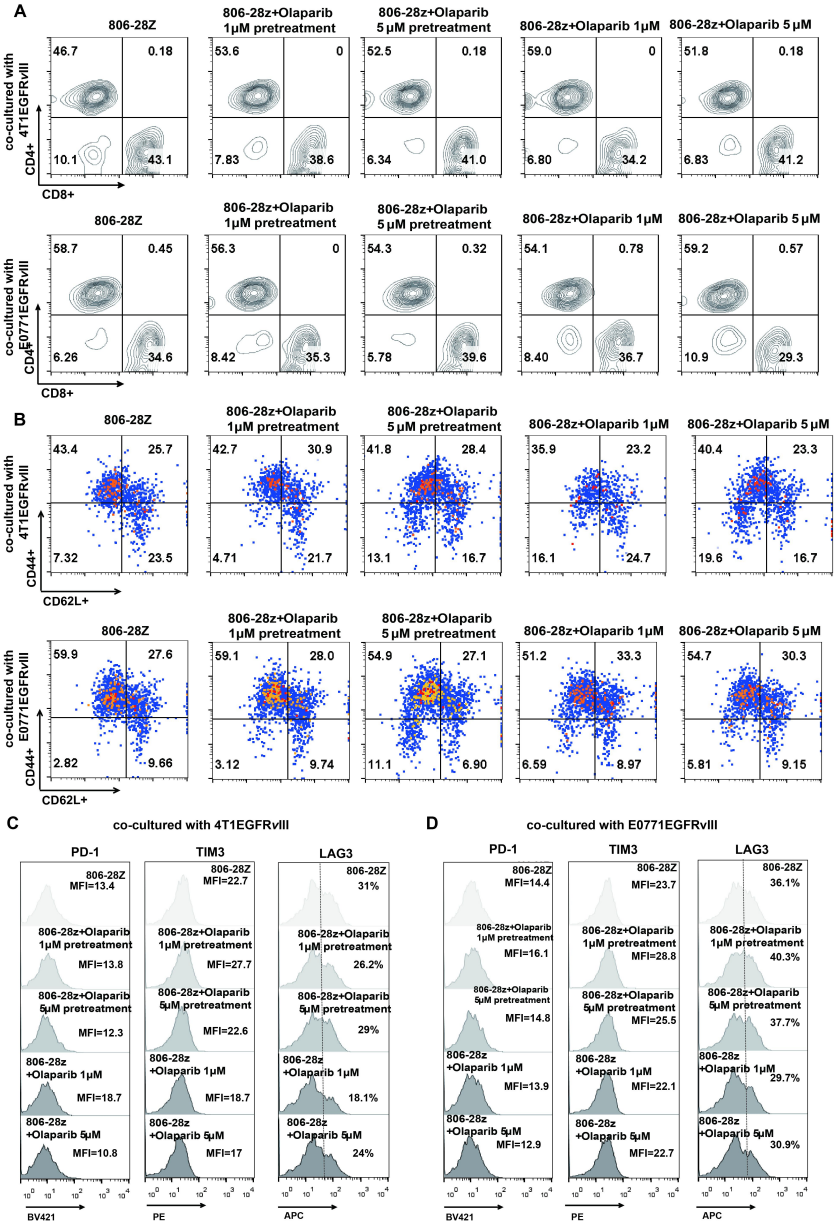

Fig. S2 The effect of olaparib on the phenotype of CAR-T cells in response to antigen stimulation

EGFR*v*III-positive tumor cells were pre-treated with or without various concentrations of olaparib for 24 h. Then, 1×10^5 CellTrace-labeled CAR-T cells were incubated with EGFR*v*III-positive tumor cells at a E/T ratio of 1:1 in the presence of indicated concentrations of olaparib for 24 h. (A) The representative flow cytometry plots results showing the frequencies of $CD4^+$ T and $CD8^+$ T cells in $CD3^+$ CAR-T cells. (B) The percentages of T_{cm} ($CD44^+CD62L^+$) in $CD8^+$ T cells of CAR-T cells in each treatment group. (C) The expression of PD1, TIM3 and LAG3 of CAR-T cells in each treatment group.

Fig. S3

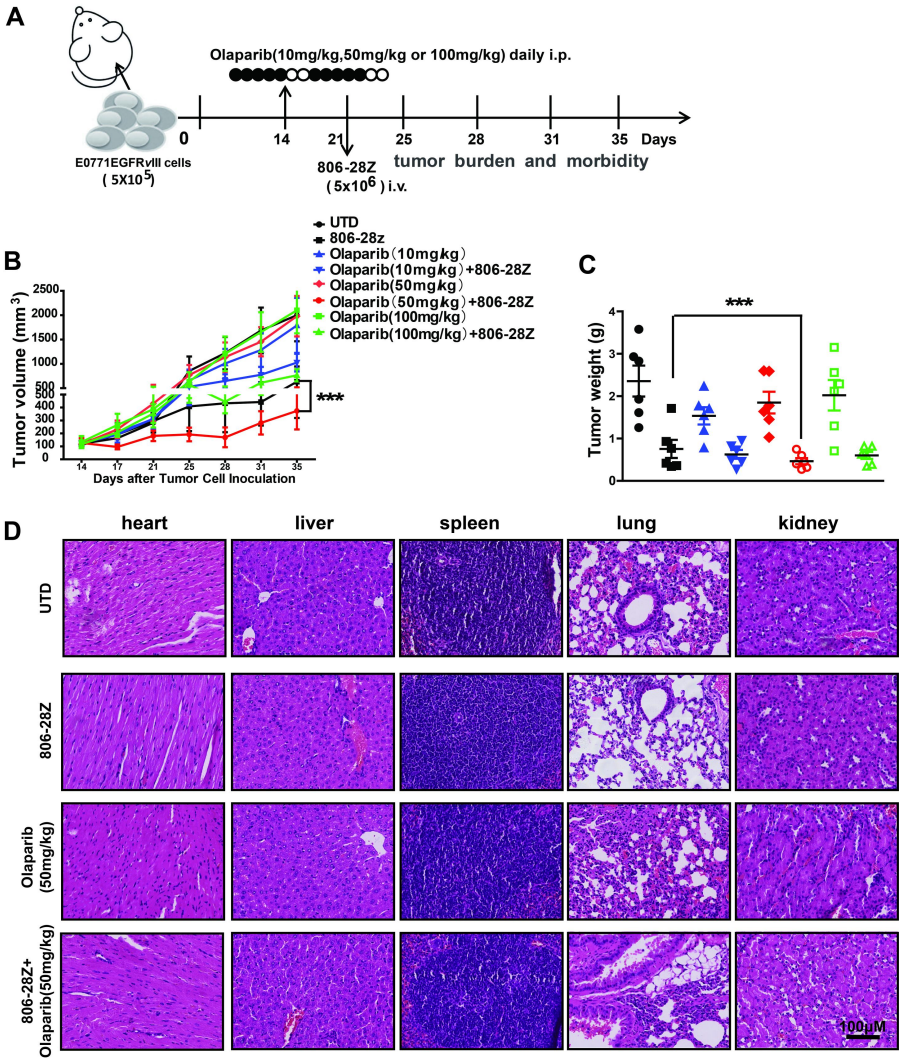

Fig. S3 The anti-tumor activity of different dose of olaparib combined with CAR-T cells in mice bearing E0771EGFR*v*III tumor cells

(A) *In vivo* experimental design. 5×10^5 EGFR*v*III-positive tumor cells were *in situ* inoculated into the forth inguinal mammary fat pads of C57BL/6 mice. Mice were administrated with various concentrations of olaparib (10mg/kg, 50mg/kg or 100mg/kg) for 10 days. Then, tumor-bearing mice received tail vein injection of 5×10^6 CAR-T cells in sterile PBS, while the control group received 5×10^6 UTD cells at day 21. (B) The average tumor growth of each treatment group. (C) The tumor weight of each treatment group. (D) The H&E staining results of heart, liver, spleen, lung and kidney of mice from each group. Scale bars, 100μm. All data are presented as the mean±SEM of triplicate experiments. ***p<0.001

Fig. S4

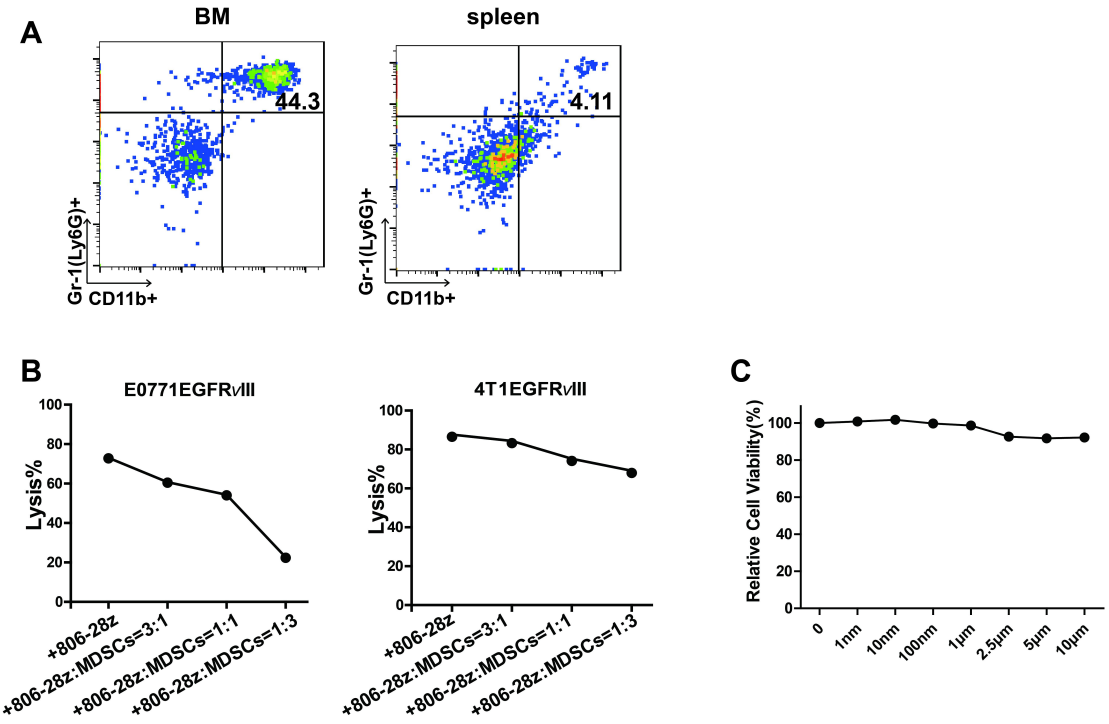

Fig. S4 *In vitro* lytic activity of CAR-T cells against EGFR*v*III-positive tumor cells co-cultured with MDSCs

(A) The representative flow cytometry plots results showing the frequencies of MDSCs ($CD11b^+Gr1^+$ cells) in $CD45^+$ immune cells isolated from bone marrow and spleen. (B) In *vitro* lytic activity of CAR-T cells against E0771EGFR*v*III and 4T1EGFR*v*III cells co-cultured with MDSCs. CAR-T cells and target cells were co-cultured at an E:T ratio of 1:1. Isolated MDSCs were added at different MDSC: CAR-T cell ratios of 1:3, 1:1, 3:1 in E-plate at 37°C for 18 h. The cytotoxicity of CAR-T cells was analyzed using a standard formula provided in the manual. (C) The cytotoxicity of olaparib to MDSCs was shown after treatment with the indicated concentrations of olaparib for 24 h by CCK8.

Fig. S5

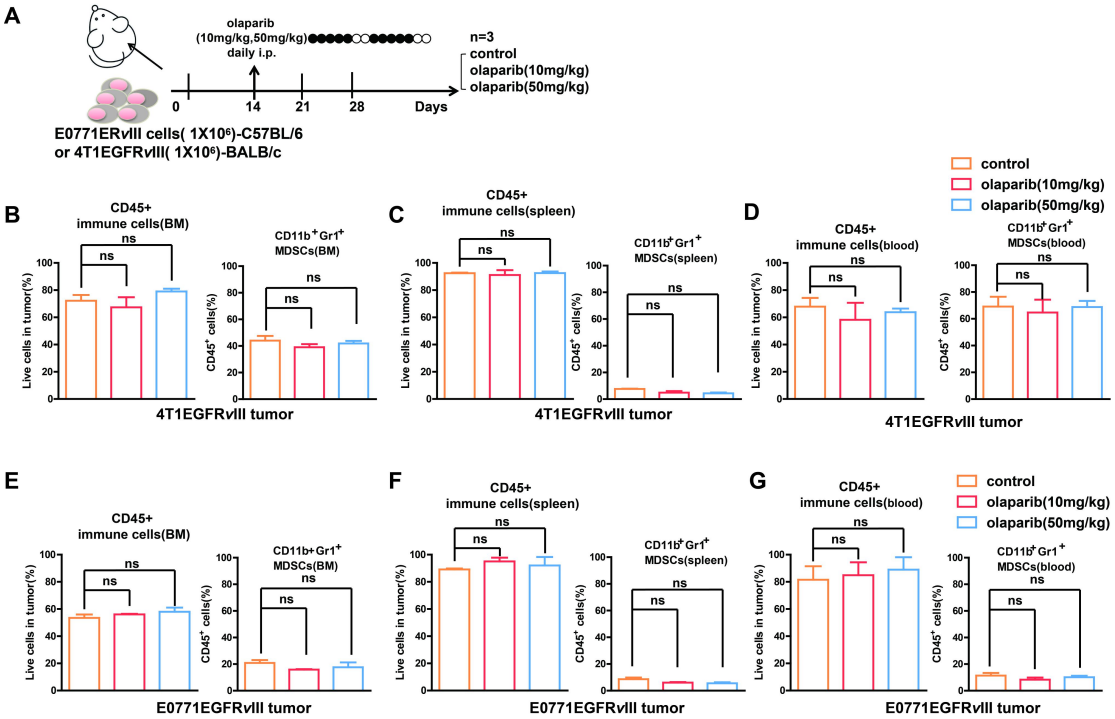

Fig. S5 The direct toxic effect of olaparib on MDSCs *in vivo*

(A) *In vivo* experimental design of EGFR*v*III-positive tumor xenografts. 1×10^6 EGFR*v*III-positive tumor cells were inoculated into the forth inguinal mammary fat pads of C57BL/6 and BABL/c mice. When the tumor volume reached 120mm^3 (day 14), tumor-bearing mice were randomly grouped. Mice were injected with 10mg/kg or 50mg/kg olaparib intraperitoneally for 10 days. (B-D) The quantitation of CD45$^+$ immune cells and MDSCs in various organs: (B) bone marrow, (C) spleen and (D) blood of 4T1EGFR*v*III tumor-bearing mice injected with different dose of olaparib. (E-G) The quantitation of CD45$^+$ immune cells and MDSCs in various organs: (E) bone marrow, (F) spleen and (G) blood of E0771EGFR*v*III tumor-bearing mice injected with different dose of olaparib. All data are presented as the mean±SEM of triplicate experiments. ns, not significant.

Fig. S6

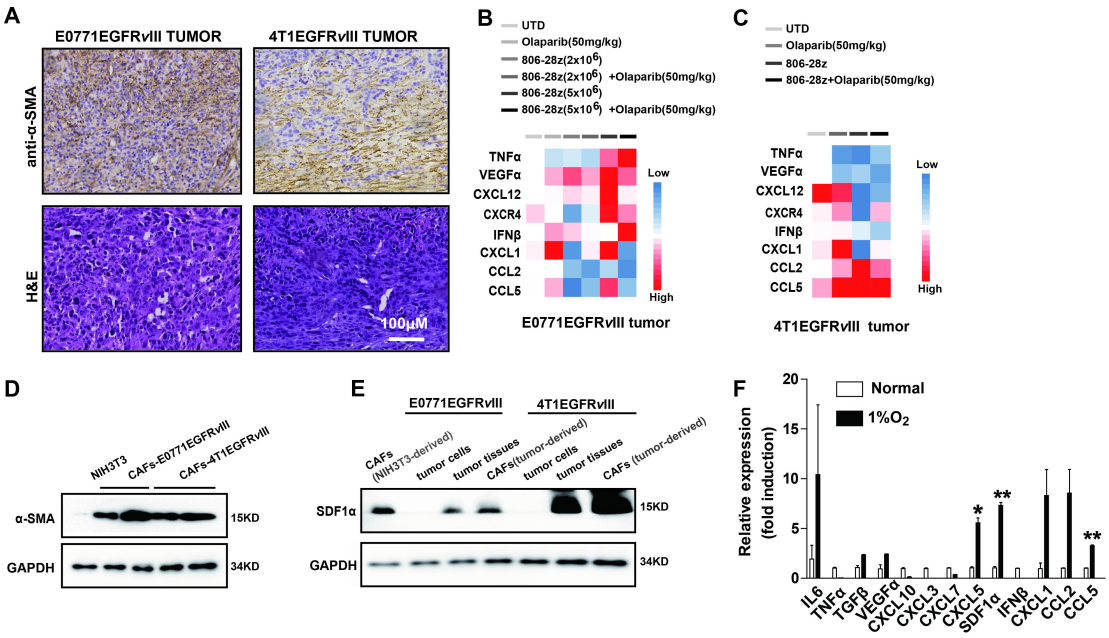

Fig. S6 SDF1α in tumor tissues mainly derived from CAFs

(A) The immunostaining images of α-SMA and H&E staining of tumor tissue from mice bearing EGFR*v*III-positive tumors. Scale bars, 100μm. (B and C) The mRNA expression of cytokines and chemokines in EGFR*v*III-positive tumor tissues of mice from each treatment group. (D) The protein levels of α-SMA and GAPDH were determined in NIH3T3 cells and CAFs isolated from tumor tissue of EGFR*v*III-positive tumor bearing mice. GAPDH served as a loading control. (E) The protein levels of SDF1α and GAPDH were determined in CAFs (induced from NIH3T3 cells), EGFR*v*III-positive tumor cells, EGFR*v*III-positive tumor tissue and CAFs isolated from tumor tissue of EGFR*v*III-positive tumor bearing mice. NIH3T3 cells were starved for 24h and then treated with TGFβ (2.5ng/ml) for 16h to acquire the phenotype of CAFs. GAPDH served as a loading control.

Fig. S7

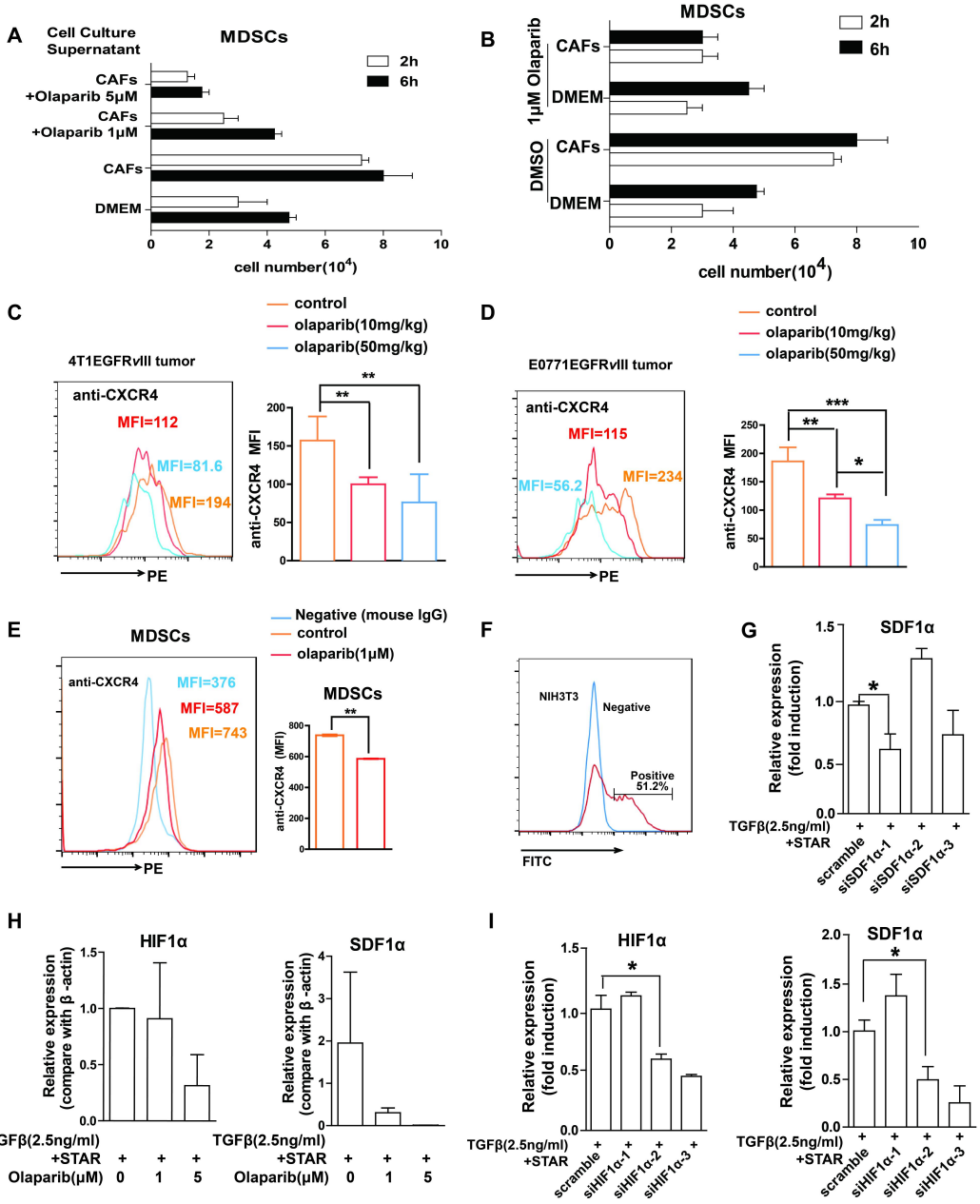

Fig. S7 Effects of olaparib on SDF1α-induced chemotaxis of MDSCs

(A) Effects of olaparib on CAFs-induced chemotaxis of MDSCs. (B) Effects of olaparib on CXCR4-dependent chemotaxis of MDSCs. MDSCs (2×10^5) treated with 1μM olaparib or DMSO for 24 were added in the upper. The cell culture supernatants of CAFs were putted in the lower chamber. The chamber aperture is 3μm. The cell number in the lower chamber was counted at 2h and 6h. (C and D) 1×10^6 EGFR*v*III-positive tumor cells were inoculated into the forth inguinal mammary fat pads of C57BL/6 and BABL/c mice. When the tumor volume reached 120mm^3 (day

14), tumor-bearing mice were randomly grouped (n=3). Then mice were injected with 10mg/kg or 50mg/kg olaparib for 10 days. The expression and quantification results of CXCR4 on MDSCs were determined by flow cytometry in tumor tissue of EGFR*v*III-positive tumor-bearing mice. (E) The expression CXCR4 on the cell surface of MDSCs treated with 1μM olaparib or DMSO (control) for 24h *in vitro* was determined by flow cytometry. Negative: mouse IgG. The numbers above the graphs indicate the MFI of CXCR4. (F) The NIH3T3 cells were transfected with control siRNA (GFP-tag) for 48h. The transfection efficiency of siRNA in NIH3T3 cells was determined by flow cytometry. (G) The CAFs were transfected with siRNA of SDF1α-1, SDF1α-2, SDF1α-3 for 48h. The mRNA expression of SDF1α was determined by Western Blot. (H) The mRNA expression of HIF1α and SDF1α in CAFs treated with 0, 1μM or 5μM olaparib for 48h. (I) The CAFs were transfected with siRNA of HIF1α for 48h. The mRNA expression of HIF1α and SDF1α was determined by RT-qPCR. All data are presented as the mean±SEM of triplicate experiments. *$p<0.05$, **$p<0.01$, ***$p<0.001$.

SUPPLEMENTARY TABLE S1 Primer sequences for various mouse genes for RT-qPCR. Primers were designed using Primer5 software

Gene	**Forward（5'-3'）**	**Reverse（5'-3'）**
UCP1	CCCGACAACTTCCGAAGTGCA	GGAAGCCTGGCCTTCACCTTG
HK1	AGGAAGAACCAACCCACAAAAC	ACCCCAAGGAAACACCACTC
HK2	GGAGGAGATGCGTAATGTGG	TGCCAGGGTTGAGAGAGAG
CPT1b	ACCACAAAGGTCGCTTCTTC	TCTTCATCCAGGGTCACAAAG
CPT2	CTCATCCGCTTTGTTCCTTC	AGTTCATCACGACTGGGTTTG
HSL	TGAGATGGTAACTGTGAGCC	ACTGAGATTGAGGTGCTGTC
ATGL	GAGCCCCGGGGTGGAACAAGAT	AAAAGGTGGTGGGCAGGAGTAAGG
PGC1α	TGCCCCTGCCAGTCACAGGA	GCTCAGCCGAGGACACGAGG
FAS	ACAAACTGCACCCTGACCCAGA	TGCTGGTTGCTGTGCATGGCT
ACC	GAAGTCAGAGCCACGGCACA	GGCAATCTCAGTTCAAGCCAGTC
PKM2	GGAGATGTGGTCATTGTGCTG	AAAGGATAGGGGAGGGGAAG
SREBP-1c	GCTTAGCCTCTACACCAACTGGC	ACAGACTGGTACGGGCCACAAG
PPARα	CAGGAGAGCAGGGATTTGCA	CCTACGCTCAGCCCTCTTCAT
FOXO1	GGACAGCCGCGCAAGACCAG	TTGAATTCTTCCAGCCCGCCGA
GSK-3β	CTGGTGCTGGACTATGTTCC	CGATGGCAGATTCCAAAGGA
iNOS	GTTCTCAGCCCAACAATACAAGA	GTGGACGGGTCGATGTCAC
CCL2	TAAAAACCTGGATCGGAACCAAA	GCATTAGCTTCAGATTTACGGGT
IL-1β	GAAATGCCACCTTTTGACAGTG	TGGATGCTCTCATCAGGACAG
IL-6	GAACAACGATGATGCACTTGC	TCTCTGAAGGACTCTGGCTTTG
TNFα	CCATTCCTGAGTTCTGCAAAGG	AAGTAGGAAGGCCTGAGATCTTATC
CCL2	GCTCAGCCAG ATGCAGTTA	CTGCTGGTGATCCTCTTGTA G
CXCL1	GCTGGGATTCACCTCAAGAA	TGGCTATGAC TTCGGTTTGG
BRCA1	ATGGATTTATCTGCCGTC	CTCAGCAGCTCTTCAGCA
BRCA2	ATGCCCGTTGAATACAAAAG	CTCTGAAAGGCGACTGGT
VEGFα	GGAGACTCTTCGAGGAGCACTT	GGCGATTTAGCAGCAGATATAAGAA
GLUT4	CTTCTTTGAGATTGGCCCTGG	AGGTGAAGATGAAGAAGCCAAGC

FATP1	TGCCTCTGCCTTGATCTTTT	GGAACCGTGGATGAACCTAA
ARG-1	AGTCTGGCAGTTGGAAGCAT	CATCTGGGAACTTTCCTTTC
CCL5	CCCACGTCAAGGAGTATTTC	ACCCTCTATCCTAGCTCATC
18s rRNA	CGGCTACCACATCCAAGGAA	GCTGGAATTACCGCGGCT
SDF1α	GGTTCTTCGAGAGCCACATC	TCTTCAGCCGTGCAACAA

SUPPLEMENTARY TABLE S2 The sequences for siRNA

siRNA	**Sense（5'-3'）**	**Anti-sense（5'-3'）**
siRNA1 HIF1α	GCUCACCAUCAGUUAUUUA TT	UAAAUAACUGAUGGUGAGC TT
siRNA2 HIF1α	CCAUGUGACCAUGAGGAAA TT	UUUCCUCAUGGUCACAUGG TT
siRNA3 HIF1α	GCUGAUUUGUGAACCCAUU TT	AAUGGGUUCACAAAUCAGC TT
siRNA1 SDF1α	GCACGGCUGAAGAACAACA TT	UGUUGUUCUUCAGCCGUGC TT
siRNA2 SDF1α	GAGUACCUGGAGAAAGCUU TT	AAGCUUUCUCCAGGUACUC TT
siRNA3 SDF1α	UCUGCAUCAGUGACGGUAA TT	UUACCGUCACUGAUGCAGA TT
Negative control	UUCUCCGAACGUGUCACGU TT	ACGUGACACGUUCGGAGAA TT